EXPERIMENTAL and MOLECULAR MEDICINE, Vol. 37, No. 3, 169-178, June 2005

Modulation of the caveolin-3 and Akt status in caveolae by insulin resistance in H9c2 cardiomyoblasts

Hyunil Ha[1] and Yunbae Pak[1,2]

[1]Department of Biochemistry
Division of Life Science
College of Natural Sciences
Graduate School of Applied Life Science
Gyeongsang National University
Jinju 660-701, Korea
[2]Corresponding author: Tel, 82-55-751-5961;
Fax, 82-55-752-7062; E-mail, ybpak@nongae.gsnu.ac.kr

Accepted 29 April 2005

Abbreviations: Akt, protein kinase B; Erk, extracellular signal related protein kinase; FITC, fluorescein isothiocyanate; GLUT4, glucose transporter 4; NIDDM, non-insulin-dependent diabetes mellitus

Abstract

We investigated glucose uptake and the translocation of Akt and caveolin-3 in response to insulin in H9c2 cardiomyoblasts exposed to an experimental insulin resistance condition of 100 nM insulin in a 25 mM glucose containing media for 24 h. The cells under the insulin resistance condition exhibited a decrease in insulin-stimulated 2-deoxy[^{3}H]glucose uptake as compared to control cells grown in 5 mM glucose media. In addition to a reduction in insulin-induced Akt translocation to membranes, we observed a significant decrease in insulin-stimulated membrane association of phosphorylated Akt with a consequent increase of the cytosolic pool. Actin remodeling in response to insulin was also greatly retarded in the cells. When translocation of Akt and caveolin-3 to caveolae was examined, the insulin resistance condition attenuated localization of Akt and caveolin-3 to caveolae from cytosol. As a result, insulin-stimulated Akt activation in caveolae was significantly decreased. Taken together, our data indicate that the decrease of glucose uptake into the cells is related to their reduced levels of caveolin-3, Akt and phosphorylated Akt in caveolae. We conclude that the insulin resistance condition induced the retardation of their translocation to caveolae and in turn caused an attenuation in insulin signaling, namely activation of Akt in caveolae for glucose uptake into H9c2 cardiomyoblasts.

Keywords: Akt; caveolae; caveolin-3; glucose uptake; H9c2 cardiomyoblasts; insulin resistance

Introduction

Type 2 or non-insulin-dependent diabetes mellitus (NIDDM) is characterized by resistance to insulin action on glucose uptake in peripheral tissues, especially skeletal muscle and adipocytes (Kahn, 1998). As defects in insulin action precede the overt disease, increased insulin secretion initially compensates for insulin resistance but overt disease occurs over time as cell compensation fails. Insulin stimulates glucose uptake into muscle and adipose tissues by affecting the redistribution of the insulin-responsive glucose transporter 4 (GLUT4) from intracellular stores to the plasma membrane to increase glucose influx (Czech and Corvera, 1999). This mechanism is abnormally diminished in type 2 diabetes, resulting in insulin resistance (Mueckler, 2001).

Insulin transmits its signals through a cell surface tyrosine kinase receptor which stimulates multiple intracellular signaling events. Activated insulin receptors phosphorylate adapter proteins, such as insulin receptor substrates, which recruit and activate downstream effector molecules. One of these proteins, phosphatidylinositol (PI) 3-kinase, is requisite for insulin regulation of glucose metabolism, especially GLUT4 translocation and glucose uptake (Sharma *et al.,* 1998). Recent studies suggest a role for Akt (protein kinase B or PKB) as a mediator of PI 3-kinase metabolic effectors (Bellacosa *et al.,* 1991; Jones *et al.,* 1991). Akt is activated by insulin and other growth factors in a variety of cell types in a manner dependent on PI 3-kinase (Franke *et al.,* 1997). Expression of constitutively active forms of Akt in appropriate tissues stimulates glucose uptake, GLUT4 translocation, glycogen synthesis, lipogenesis, and protein synthesis (Cong *et al.,* 1997; Tanti *et al.,* 1997; Kohn *et al.,* 1998; Ueki *et al.,* 1998; Hajduch *et al.,* 2001).

Recent reports showed that insulin receptors are sequestered in caveolae of the adipocyte plasma membrane, and suggest that caveolae are critical for insulin action (Yamamoto *et al.,* 1998; Gustavsson *et al.,* 1999; Bickel, 2002; Cohen *et al.,* 2003a; b). As recently reviewed in detail (Razani *et al.,* 2002; Gratton *et al.,* 2004), caveolae invaginations are found in the plasma membrane of many cell types, but are

most abundant in endothelial and epithelial cells, adipocytes, fibroblasts, and myocytes. Caveolae are formed from cholesterol- and sphingolipid-rich rafts in plasma membrane in a process requiring the caveolae-specific structural protein caveolin. Caveolin is found in plasma membrane and intracellularly, but in plasma membrane is confined to caveolae. It is therefore used as a marker for these structures (Schlegel *et al.,* 1998). Molecular cloning has identified three distinct caveolin genes, caveolin- 1, -2 and -3. In contrast to caveolin-1 and -2 which are most abundantly expressed in adipocytes, endothelial cells and fibroblastic cell types, caveolin-3 expression is mostly confined to striated (cardiac and skeletal) and smooth muscle. Caveolin-3 in muscle cells has been shown to be responsible for organelle biogenesis in these tissues and caveolin-3 null mice lack caveolae only in these tissues (Hagiwara *et al.,* 2000; Galbiati *et al.,* 2002).

Recent studies have suggested regulatory as well as structural functions for caveolin, which may directly regulate numerous signaling proteins in caveolae (Razani *et al.,* 2002; Cohen *et al.,* 2003b; Ha *et al.,* 2003; Gratton *et al.,* 2004; Kim *et al.,* 2004; Kim and Pak, 2005). Different groups have demonstrated inhibition of G proteins, Src family kinases, nitric oxide synthase, epidermal growth factor receptor, MAP kinase, and protein kinase C by a caveolin scaffolding domain, leading to the suggestion that the biological function of caveolin in caveolae is to suppress cellular signaling (Uttenbogaard *et al.,* 2000; Liu *et al.,* 2002; Razani *et al.,* 2002; Cohen *et al.,* 2003b; Gratton *et al.,* 2004). The specificity of caveolin interaction with these molecules has been confirmed by identifying a common amino acid sequence motif contained in many of these regulatory molecules and in the insulin receptor (IR) as well (Cohen *et al.,* 2003b; Gratton *et al.,* 2004).

Using H9c2 cardiomyoblasts, we examined whether insulin resistance modulates insulin responses and subsequent downstream signal cascades, such as glucose uptake, activation of Akt and Erk, actin remodeling, and translocation of caveolin-3 and Akt to caveolae. To induce an experimental condition of insulin resistance, H9c2 cells were grown in high glucose (25 mM) plus high insulin (100 nM)-containing media for 24 h (Thomson *et al.,* 1997; Tong *et al.,* 2001). Akt activation and its translocation to caveolae in response to insulin was then investigated by subcellular fractionation, sucrose gradient caveolar enriched membrane fractionation, glucose uptake measurements and immunofluorescence microscopy for analysis of actin remodeling. We report that the insulin resistance condition decreases Akt translocation to caveolae, insulin-stimulated Akt activation in caveolae, and 2-deoxy[^{3}H]glucose uptake with an impairment of insulin-induced actin remodeling in H9c2 cardiomyoblast cells.

Materials and Methods

Cell culture

H9c2 (a cardiomyoblast cell line derived from embryonic rat heart tissue) cells (Kimes and Brandt, 1976; Levy *et al.,* 1996) were maintained in Dulbecco's modified Eagle's medium (DMEM) (GIBCO/BRL) containing 5 mM glucose supplemented with 10% fetal bovine serum (FBS) (Hyclone, Logan, Utah), penicillin (100 U/ml) (Sigma Chemical Co., St. Louis, MO) and streptomycin (100 μg/ml) (Sigma) at 37°C under an atmosphere of 95% air and 5% CO_2. To test an experimental hyperglycemic condition, cells were incubated in DMEM containing 25 mM glucose supplemented with 10% FBS, penicillin (100 U/ml) and streptomycin (100 μg/ml) for 0.5 or 24 h. Cells were serum starved for 24 h in DMEM containing 5 mM (control) or 25 mM (hyperglycemic condition) glucose, supplemented with 0.5% bovine serum albumin (BSA) (Fraction V; Sigma) and then compared to each other by incubating with or without 100 nM insulin (Porcine, Sigma I0259) for 10 min. To investigate an experimental condition of insulin resistance, cells were incubated for 24 h in DMEM supplemented with 10% FBS containing 5 mM glucose (control) or 25 mM glucose plus 100 nM insulin (insulin resistance condition) (Thomson *et al.,* 1997; Tong *et al.,* 2001) prior to serum starvation for 4 h in DMEM supplemented with 0.5% BSA, and treated with or without 100 nM insulin for 5-15 min.

Western blot analysis

Protein extracts were generated from cells using RIPA buffer (50 mM HEPES, 150 mM NaCl, 100 mM Tris-HCl, pH 8.0, 1% Triton X-100, 1% deoxycholic acid, 0.1% SDS, 5 mM EDTA), containing 10 mM NaF, 5 mM DTT, 1 mM phenylmethylsulfonyl fluoride (PMSF), 1 mM sodium vanadate, 20 μM leupeptin, and 100 μM aprotinin. Equal amounts of samples (15-40 μg) were subjected to SDS-polyacrylamide gel electrophoresis (PAGE), transferred to polyvinylidene difluoride (PVDF) membrane (Millipore; Bedford, MA) at 350 mA for 2 h using the BIO-RAD transfer system. The membrane was blocked in 5% non-fat dry milk in TBS-T buffer (10 mM Tris-HCl, pH 8.0, 150 mM NaCl with 0.1% Tween 20). Primary antibodies were incubated for 1 h at room temperature in above blocking buffer. The membrane was then washed for 30 min, with TBS-T buffer changed every 5 min before 1 h of incubation in IgG-horseradish peroxidase (Promega, W4011, W4021) at a final titer of 1:2500 at room temperature. The washes were repeated before the membrane was developed with a light-emitting nonradioactive method using ECL reagent (Amersham, Arlington Heights, IL). The membrane was then subjected to autoluminography for 1 to 5 min and scanned. The primary antibodies used for our experiments were anti-caveolin-1 (Transduction Laboratories, C37120 mAb; 1:1,000 dilution), anti-caveoiln-2 (Transduction Laboratories, C57820

mAb; 1:250 dilution), anti-caveoiln-3 (Transduction Laboratories, C38320 mAb; 1:5,000 dilution), anti-Erk (Transduction Laboratories, M12320 mAb; 1:5,000 dilution), anti-phosphospecific-Erk (Thr 202 and Tyr 204) (New England Biolabs., 9106S mAb; 1:2,000 dilution), anti-Akt (Transduction Laboratories, P67220 mAb; 1:500 dilution), and anti-phosphospecific-Akt (Ser 473) (New England Biolabs., 9271L pAb; 1:1000 dilution) antibodies.

Cytosol and membrane fractionation

Cells were washed twice in phosphate-buffered saline (PBS) and then homogenized in homogenization buffer (150 mM NaCl, 1 mM EGTA, 0.1 mM $MgCl_2$, 10 mM HEPES, pH 7.4) containing phosphatase and protease inhibitors (2 mM sodium orthovanadate, 10 mM NaF, 1 mM tetra-sodium pyrophosphate, 10 μg/ml leupeptin, 250 μM PMSF) and subjected to subcellular fractionation as described previously (Yu *et al.,* 1999) with the following modification. Cell homogenates were centrifuged for 5 min at 200 *g* to remove nuclei. The resulting supernatant was then centrifuged at 16,000 *g* for 15 min yielding a plasma membrane-containing pellet (membrane fraction). The supernatant, representing the cytosolic fraction was concentrated. The membrane and cytosolic fractions were then subjected to immunoblotting for Akt and phosphorylated Akt.

2-Deoxy[^{3}H]glucose uptake

Glucose uptake was assayed by accumulation of 2-deoxy-D-[1-^{3}H]glucose (Amersham, Arlington Heights, IL) as described previously (Kotani *et al.,* 1998). In brief, confluent H9c2 cells in 12-well plates were washed twice with DB buffer (140 mM NaCl, 2.7 mM KCl, 1 mM $CaCl_2$, 1.5 mM KH_2PO_4, 8 mM Na_2HPO_4, pH 7.4, 0.5 mM $MgCl_2$) containing 0.2% BSA and incubated in DB buffer for 30 min at 37°C. Insulin was added to a final concentration of 100 nM and cells were further incubated for 15 min. Finally, DB buffer containing 0.2% BSA and 0.05 mM 2-deoxy[^{3}H] glucose (0.5 μCi) was added to each well, and after 5 min incubation, cells were washed three times with ice-cold PBS and then solubilized with 0.1% (w/v) SDS. The radioactivity incorporated into the cells was measured with a liquid scintillation counter (Beckman Instruments, Palo Alto, CA).

Immunolabeling and immunofluorescence microscopy

H9c2 cells grown on glass coverslips were incubated for 24 h in DMEM containing 25 mM glucose plus 100 nM insulin before serum starvation for 4 h. Serum-starved cells were then stimulated with 100 nM insulin for 15 min, washed three times with PBS, and fixed for 30 min at room temperature with 3.7% formaldehyde in PBS. Fixed cells were rinsed with PBS and permeabilized with PBS containing 0.1% Triton X-100 and 0.2% BSA for 10 min. Cells were then treated with 25 mM NH_4Cl in PBS for 10 min at room temperature to quench free aldehyde groups. Cells were rinsed again with PBS and incubated with phalloidin-fluorescein isothiocyanate (FITC)-conjugated anti-mouse IgG antibody (1:100) (Jackson Immuno-Research Laboratories Inc.) diluted in PBS with 0.1% Triton X-100 and 0.2% BSA to stain F-actin for 1 h at room temperature. After three washes for 10 min each with PBS, cells were then viewed by immunofluorescence microscopy (Olympus BX51 microscope with Olympus PM-20 exposure control unit) as previously described (Kim and Pak, 2005).

Isolation of caveolae

Caveolae fractions were prepared without detergent as described previously (Song *et al.,* 1996; Rybin *et al.,* 2000; Karlsson *et al.,* 2002). Briefly, cells from two 150-mm diameter dishes were washed twice with ice-cold PBS and harvested with 0.5 M Na_2CO_3 buffer, pH 11.0. Subsequent procedures were carried out at 4°C. To disrupt cellular membranes, homogenization was carried out with a loose fitting Dounce homogenizer (10 strokes). The homogenate was then adjusted to 40% sucrose by adding an equal volume of 80% sucrose prepared in Mes-buffered saline (25 mM Mes, pH 6.5, 0.15 M NaCl), placed on the bottom of an ultracentrifuge tube, overlaid with a 5-35% discontinuous sucrose gradient (4 ml of 5% sucrose, 4 ml of 35% sucrose; both in Mes-buffered saline containing 250 mM Na_2CO_3), and centrifuged at 39,000 *g* for 18 h in a SW41 rotor (Beckman Instruments, Palo Alto, CA). After centrifugation, proteins in each of the twelve 1-ml gradient fractions were concentrated by precipitation with trichloroacetic acid (TCA) as follows. Fractions were mixed with 20% TCA (v/v) and incubated for 30 min on ice. Precipitated proteins were pelleted by centrifugation at 3,700 *g* for 15 min at 4°C. Each pellet from the fractions was washed three times with 1 ml of ice-cold 80% ethanol and dissolved in SDS-PAGE sample buffer for SDS-PAGE and immunoblotting for caveolin-3 and Akt. For the analysis of insulin-stimulated translocation of Akt and caveolin-3 to the isolated caveolae, aliquots of proteins pooled from the caveolin-3 rich membrane fractions designated as fractions 4, 5, and 6 were collected from the light-scattering band at the 5-35% sucrose interface and subjected to SDS-PAGE and immunoblotting for caveolin-3, Akt, and phosphorylated Akt.

Densitometry analysis

Autoradiograms were quantified with an imaging densitometer using the Molecular Analyst software (Bio-Rad Laboratories, model GS-700). Signal intensities of bands in immunoblots were determined by the scanning laser densitometry.

Results

Effect of hyperglycemia on activation of Erk and Akt, and 2-deoxy[^{3}H]glucose uptake

Since hyperglycemia is not only a consequence of, but also an important factor in worsening both insulin resistance and insulin deficiency, we first investigated the effect of hyperglycemia on Erk and Akt activation, and glucose uptake in response to insulin in H9c2 cells. Activation of Erk and Akt was assessed by immunoblotting with anti-phosphospecific antibodies directed against Thr 202 and Tyr 204 of Erk and Ser 473 of Akt, respectively.

When control cells grown in 5 mM glucose media were treated with insulin, marked increases in insulin-induced phosphorylation of both Erk and Akt was observed (Figure 1A, lanes 1 and 2). Cells grown in the experimental hyperglycemic condition for 24 h, however, exhibited no significant differences in the insulin-stimulated Erk and Akt activation (Figure 1A, lanes 3 and 4) as compared to controls. In addition, when we examined the effect of long-term (24 h) *vs* short-term (0.5 h) incubation of cells in the hyperglycemic condition, a similar pattern of activation was observed except for a relative increase in the basal level of Akt activation in 0.5 h incubation (Figure 1A, lanes 3 and 4 *vs* 5 and 6). Relative increases in the insulin-stimulated Akt activation was detected in cells under the hyperglycemic condition compared to controls (Figure 1A lanes 4 and 6 *vs* 2). No significant change was observed in the expression level of either Erk or Akt between control and hyperglycemic conditions (data not shown).

When we further examined the insulin-stimulated glucose uptake, cells grown under the hyperglycemic condition for 24 h showed almost the same efficiency in both basal and insulin-stimulated 2-deoxy[^{3}H] glucose uptake as control cells (Figure 1B). This result is consistent with recent findings (Nelson *et al.,* 2000; Kawanaka *et al.,* 2001) demonstrating that high glucose treatment alone does not impair insulin-induced glucose uptake in adipocyte and muscle.

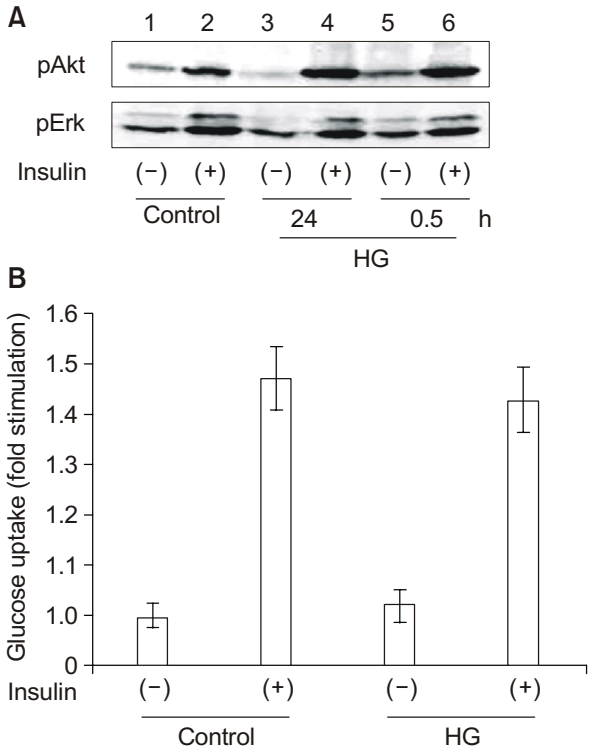

Figure 1. Effect of hyperglycemia on activation of Akt and Erk, and 2-deoxy[^{3}H]glucose uptake in response to insulin. (A) H9c2 cells were preincubated for 24 h in serum-starved DMEM containing 5 mM (control) or 25 mM glucose (hyperglycemic condition; HG). Cells were then stimulated with 100 nM insulin for 10 min. Some cells were preincubated for 0.5 h in the serum-starved media containing 25 mM glucose and stimulated with 100 nM insulin for 10 min to compare with 0.5 h and 24 h incubation of cells under the hyperglycemic condition. Whole cell lysates were subjected to SDS-PAGE and immunoblotted with anti-phosphospecific-Akt (Ser 473) or anti-phospospecific-Erk (Thr 202 and Tyr 204) antibodies. (B) H9c2 cells were serum-starved in DMEM containing 5 mM or 25 mM glucose for 24 h and stimulated with or without 100 nM insulin for 15 min. Cells were then incubated with 2-deoxy[^{3}H]glucose for 5 min as described in Materials and Methods. Cells were washed three times with ice-cold PBS, and the radioactivity taken up by the cells was measured by liquid scintillation counting. Results are expressed as the fold change in the 2-deoxy[^{3}H]glucose uptake relative to basal cells in the untreated control (means ± S.E. of three independently performed experiments). $P < 0.05$ compared with respective control incubated in 5 mM glucose media.

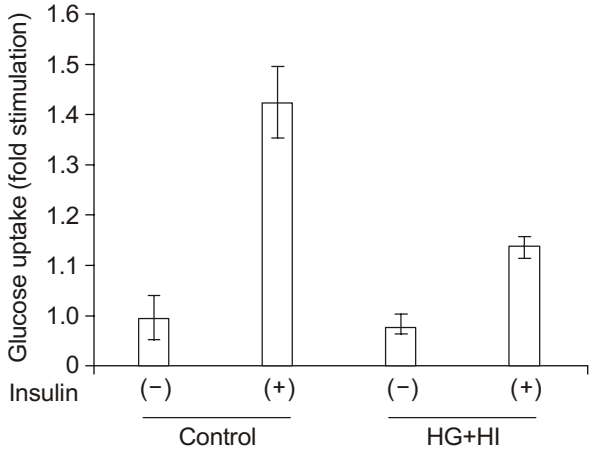

Figure 2. Effect of insulin resistance on insulin-stimulated 2-deoxy[^{3}H] glucose uptake. H9c2 cells were maintained either in DMEM containing 25 mM glucose plus 100 nM insulin (HG + HI; insulin resistance condition) or 5 mM glucose (control) for 24 h. Cells were then serum starved for 4 h before 100 nM insulin stimulation for 15 min. Quantification of glucose uptake was performed with 2-deoxy[^{3}H] glucose as in Figure 1. Results are expressed as the fold change in the 2-deoxy[^{3}H]glucose uptake relative to basal cells in the untreated control (means ± S.E. of three independently performed experiments). $P < 0.05$ compared with respective control incubated in 5 mM glucose media.

Effect of insulin resistance on 2-deoxy[^{3}H]glucose uptake

We then tested the effect of the exposure of H9c2 cells to high glucose (25 mM) plus high insulin (100 nM) condition for 24 h, an experimental strategy reported to cause insulin resistance in L6 myotubes and 3T3-L1 adipocytes (Thomson *et al.,* 1997; Tong *et al.,* 2001), to insulin-induced glucose uptake. When cells under the insulin resistance condition were treated with insulin, there was no marked change in basal uptake but the insulin-stimulated uptake of 2-deoxy[^{3}H]glucose was significantly reduced (approximately 46% stimulation *vs* 16% stimulation in insulin resistance, thus a 65% decrease in the uptake) as compared to control cells grown in 5 mM glucose alone (Figure 2). Thus, these data indicate that the experimental condition of insulin resistance caused the attenuation of insulin-stimulated glucose uptake in H9c2 cardiomyoblast cells.

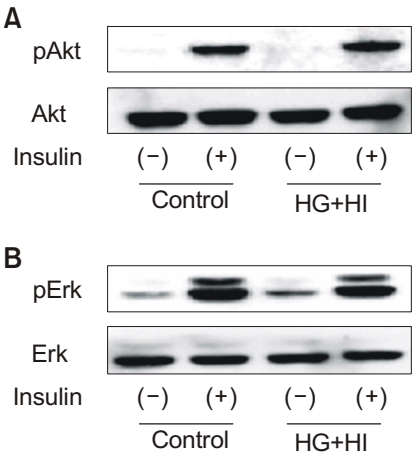

Figure 3. Effect of insulin resistance on insulin-stimulated activation of Akt and Erk. H9c2 cells were incubated either in DMEM containing 25 mM glucose plus 100 nM insulin (HG + HI; insulin resistance condition) or in 5 mM glucose (control) for 24 h and subjected to serum starvation for 4 h. Cells were then stimulated with 100 nM insulin for 5 min. Whole cell lysates were subjected to SDS-PAGE and immunoblotted with (A) anti-phosphospecific-Akt (Ser 473) or anti-Akt antibodies, and (B) anti-phospospecific-Erk (Thr 202 and Tyr 204) or anti-Erk antibodies.

Activation of Erk and Akt by insulin

To investigate the molecular mechanism by which the experimental condition of insulin resistance impairs insulin-stimulated 2-deoxy[^{3}H]glucose uptake in H9c2 cardiomyoblasts, we next examined the effect of the insulin resistance condition on the activation of Erk and Akt by insulin. When H9c2 cells exposed to the insulin resistance condition were incubated with insulin, there were no significant changes observed in both protein expression level and activation of Erk and Akt compared to control cells grown in 5 mM glucose alone (Figure 3A and B) except a slight increase in basal Erk activation (Figure 3B).

Translocation of Akt in response to insulin

Although our result showed that the insulin resistance condition caused the reduction in insulin-stimulated 2-deoxy[^{3}H]glucose uptake in H9c2 cells (Figure 2), we were unable to detect any significant difference in Akt activation at the whole cell level as compared to control (Figure 3A). Since Akt is translocated from cytosol to plasma membrane upon growth factor stimulation, and the process is suggested to be ne-

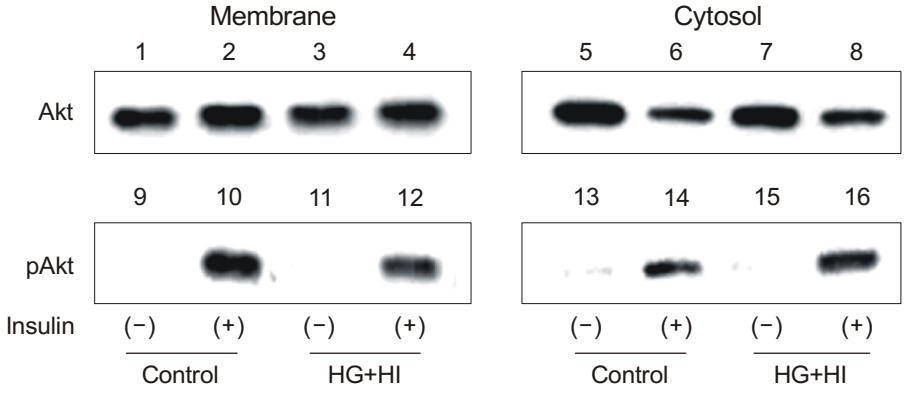

Figure 4. Effect of insulin resistance on insulin-stimulated translocation of Akt. H9c2 cells were incubated either in DMEM containing 25 mM glucose plus 100 nM insulin (HG + HI; insulin resistance condition) or in 5 mM glucose (control) for 24 h and subjected to serum starvation for 4 h. Cells were then stimulated with 100 nM insulin for 7 min. Cell homogenates were centrifuged for 5 min at 200 *g* to remove nuclei. The resulting supernatant was centrifuged at 16,000 *g* for 15 min yielding a pellet, - the plasma membrane-containing fraction. The supernatant containing cytosol was concentrated. Equal amounts of protein from the membrane and cytosolic fractions were subject to SDS-PAGE and immunoblotted with anti-Akt or anti-phosphospecific-Akt (Ser 473) antibodies.

cessary for the activation of Akt (Alessi *et al.,* 1996), we accordingly examined the insulin-stimulated cellular translocation of Akt and phosphorylated Akt between the cytosol and membrane fractions of the cells under the insulin resistance condition. Insulin induced a significant translocation of Akt from the cytosol to the membrane fraction (Figure 4, lanes 2 and 6) in control cells. These results are consistent with the previous findings of insulin-stimulated Akt translocation from cytosol to plasma membrane in adipocytes (Cong *et al.,* 1997; Tanti *et al.,* 1997). In comparison, cells under the insulin resistance condition showed similar Akt expression and pattern of Akt translocation in the fractions in response to insulin (Figure 4, lanes 3 and 7, and lanes 4 and 8) as in control cells (Figure 4, lanes 1 and 5, and lanes 2 and 6). However, a decrease in the insulin-stimulated translocation of Akt from cytosol to the membrane fraction was detected in cells under the insulin resistance condition (Figure 4, lanes 8 and 4) compared to control cells (Figure 4, lanes 6 and 2). Moreover, the insulin resistance condition reduced significantly the membrane association of phosphorylated Akt and a consequent increase of the cytosolic pool as compared to control cells (Figure 4, lanes 12 and 16 *vs* lanes 10 and 14).

Actin remodeling in response to insulin

Insulin causes a rapid remodeling of actin filaments, promoting membrane ruffling in various cells as diverse as myotubes (Tsakiridis *et al.,* 1994), adipocytes (Wang *et al.,* 1998), and fibroblasts (Clodi *et al.,* 1998). Previous studies examining the role of the actin cytoskeleton on GLUT4 translocation in L6 myotubes, 3T3-L1 adipocytes, and rat adipocytes showed that disruption of the actin cytoskeleton by either cytochalasin D or latrunculin A inhibited insulin-mediated GLUT4 translocation (Olson *et al.,* 2001). Accordingly, we examined the actin remodeling by insulin in H9c2 cells under the insulin resistance condition. An acute 100 nM insulin treatment for 15 min in control cells grown in 5 mM glucose alone induced membrane ruffling and a decrease in actin stress fiber (Figure 5). Cells grown in the insulin resistance condition, however, showed an impairment of the insulin-stimulated actin remodeling, namely in the rearrangement of actin stress fibers to the membrane ruffling formation as normally observed in control cells (Figure 5). Thus, these data suggest that the attenuation of glucose uptake in H9c2 cells (Figure 2) could be due to the retardation of actin remodeling by the insulin resistance condition.

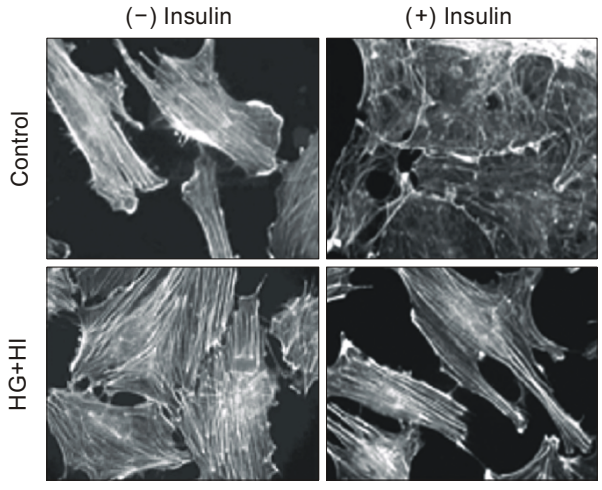

Figure 5. Insulin resistance impairs insulin-stimulated actin remodeling. H9c2 cells were grown on coverslips either in DMEM containing 25 mM glucose plus 100 nM insulin (HG + HI; insulin resistance condition) or in 5 mM glucose (control) for 24 h and subjected to serum starvation for 4 h. Cells were then stimulated with 100 nM insulin for 15 min, fixed with paraformaldehyde, detergent permeabilized, and stained for F-actin using FITC-phalloidin. The actin cytoskeleton was visualized by immunofluoresence microscopy (magnification, ×400).

Localization of caveolin-3 and Akt to caveolae

To better understand how caveolae are involved in the insulin responses in H9c2 cells, caveolar-enriched fractions were isolated by discontinuous sucrose gradient caveolin-3 enriched membrane fractionation

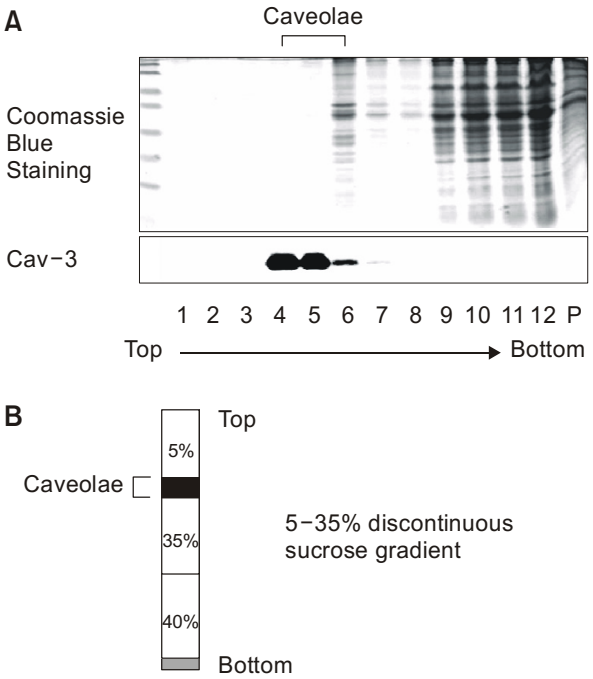

Figure 6. Fractionation and purification of caveolar-enriched fractions. Isolation of caveolar-enriched fractions was performed using a 40%, 35%, and 5% sucrose step gradient and analytical centrifugation. A flocculent and dense white band enriched in caveolae appeared at the interface between the 35 and 5% sucrose layers. Fractions were collected starting from top to bottom of the gradient, subjected to SDS-PAGE, analyzed by Coommassie blue staining, and immunoblotted with anti-caveolin-3 antibody. P, pellet.

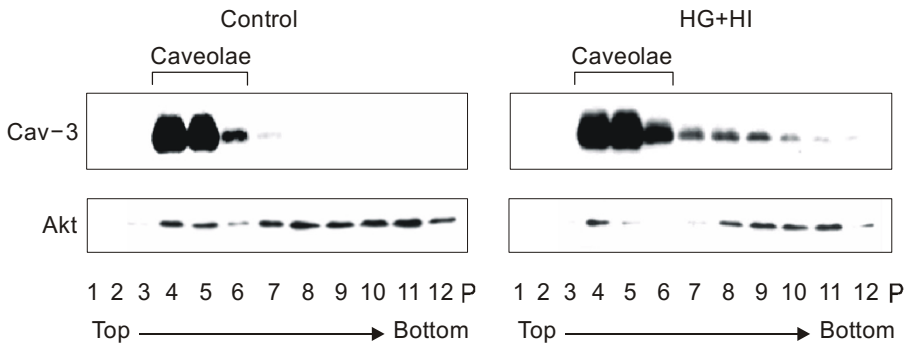

Figure 7. Insulin resistance reduces the localization of caveolin-3 and Akt to caveolae. H9c2 cells grown either in DMEM containing 25 mM glucose plus 100 nM insulin (HG + HI; insulin resistance condition) or in 5 mM glucose (control) for 24 h were lysed and subjected to caveolar enriched-fractionation using the 5-35% discontinuous sucrose gradient as described in Figure 6. Each 1-ml fraction was collected from the top of the gradient, subjected to SDS-PAGE, and immunoblotted with anti-Akt or anti-caveolin-3 antibodies.

without detergent as described in Materials and Methods. Equal aliquots of protein from each fraction were separated by SDS-PAGE. Coomassie blue staining showed that most of the cellular protein was fractionated toward the bottom 9-12 fractions and the pellet (Figure 6A and B). The caveolae fractions were collected from fractions 4-6, which were visualized as a light-scattering band at the 5-35% sucrose interface as depicted in Figure 6B. We then examined any attenuation in translocation of caveolin-3 and Akt from cytosol to caveolae in cells exposed to the insulin resistance condition (Figure 7). In control cells grown in 5 mM glucose alone, Akt was detected in caveolae (fractions 4-6) as well as in non-caveolae fractions (fractions 9-12) whereas caveolin-3 was exclusively present in caveolae (fractions 4-6) (Figure 7). Cells grown in the insulin resistance condition, however, exhibited a dispersed distribution of caveolin-3 toward bottom fractions and a significant decrease in the localization of Akt to caveolae (Figure 7). Thus, it appears that the insulin resistance condition attenuates localization of Akt and caveolin-3 to caveolae from cytosol.

Insulin-induced activation of Akt in caveolae

We then investigated the effect of insulin resistance on insulin-induced Akt activation in isolated caveolae. In control cells, insulin markedly increased the amount of phosphorylated Akt by 4.3-fold in caveolae, (Figure 8, lane 2). However, the insulin-stimulated translocation of phosphorylated Akt to caveolae was significantly reduced (approximately 60% reduction compared to control) in cells under the insulin resistance condition with only a 1.7-fold increase above the basal level (Figure 8, lane 4). Consistent with the results shown in Figure 7, the Akt and caveolin-3 protein levels in caveolae were higher in control cells (Figure 8, lanes 1and 2 *vs* lanes 3 and 4). However, no significant changes in the levels of Akt and caveolin-3 were observed in response to insulin compared to cells without insulin treatment in both controls and cells under insulin resistance condition (Figure 8, lanes 1 *vs* 2 and lanes 3 *vs* 4). These results suggest that a decreased Akt activation in caveolae paralleled the modulation of translocation of the phosphorylated forms by the insulin resistance

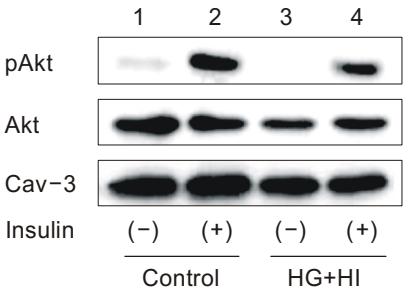

Figure 8. Effect of insulin resistance on insulin-induced activation and translocation of Akt to the isolated caveolae. H9c2 cells were incubated either in DMEM containing 25 mM glucose plus 100 nM insulin (HG+HI; insulin resistance condition) or in 5 mM glucose (control) for 24 h and serum starved for 4 h. Cells were then stimulated with 100 nM insulin for 10 min and subjected to the caveolar-enriched fractionation as shown in Figures 6 and 7. Aliquots of protein pooled from the isolated caveolae fractions (i.e., fractions 4, 5, and 6 from caveolar-enriched fractionation as shown in Figure 6) were subjected to SDS-PAGE and immunoblotted with anti-Akt, anti-phosphospecific-Akt (Ser 473), or caveolin-3 antibodies.

condition. Thus, it appears that the reduction in the translocation of caveolin-3, Akt, and phosphorylated Akt to caveolae due to insulin resistance results in the subsequent attenuation of glucose uptake.

Discussion

H9c2 is a cardiac muscle cell line that has been used to investigate heart function (Kimes and Brandt, 1976; Levy *et al.,* 1996; Yu *et al.,* 1999). H9c2 cardiomyoblasts exhibit insulin-stimulated glucose transport, although the magnitude of the stimulatory effect (approximately 1.5-fold) is less than the severalfold increases observed in skeletal muscles and adipocytes (Stephen and Pilch, 1995; Yu *et al.,* 1999). To define further the role of insulin resistance in heart, and to investigate the mechanisms involved in translocation of caveolin-3 and Akt to caveolae and glucose uptake by insulin, the effects of insulin resistance on Akt activation and translocation to caveolae, actin remodeling, and glucose uptake were evaluated in H9c2 cardiomyoblasts.

The present results indicate that the hyperglycemic condition of high glucose (25 mM) alone did not alter insulin-stimulated glucose uptake in H9c2 cells (Figure 1). In addition, no significant difference in the glucose uptake was detected when the hyperglycemic effect of long-term (24 h) *vs* short-term (0.5 h) incubation was examined (Figure 1). These results are consistent with recent studies reporting that high glucose treatment alone did not impair insulin-induced glucose uptake in adipocytes and skeletal muscle (Nelson *et al.,* 2000; Kawanaka *et al.,* 2001). However, an experimental condition of high glucose (25 mM) plus high insulin (100 nM) for 24 h exposure, demonstrated to produce insulin resistance in L6 myoblasts and 3T3-L1 adipocytes (Thomson *et al.,* 1997; Tong *et al.,* 2001), significantly decreased the insulin-stimulated glucose uptake in H9c2 cells (Figure 2). It has been shown that insulin promotes membrane ruffling by a rapid remodeling of actin filaments and that the disruption of the actin cytoskeleton inhibited insulin-mediated GLUT4 translocation in myoblasts, fibroblasts and adipocytes (Tsakiridis *et al.,* 1994; Clodi *et al.,* 1998; Wang *et al.,* 1998; Olson *et al.,* 2001; Tong *et al.,* 2001). Thus, the reduction in the insulin-stimulated glucose uptake (Figure 2) and the present results obtained from the retardation of actin remodeling by the insulin resistance condition in H9c2 cardiomyoblasts (Figure 5) are indicative that insulin resistance results in the impairment of glucose uptake in cardiac muscle.

When we investigated the effect of insulin resistance on the activation and translocation of Akt, a putative upstream regulatory signaling molecule of insulin-induced glucose uptake, there were no significant differences between basal and insulin-stimulated Akt activation in whole cell lysate (Figure 3). However, insulin-stimulated translocation of phosphorylated Akt to membrane was markedly decreased in H9c2 cells under the insulin resistance condition (Figure 4). Moreover, the insulin resistance condition dramatically reduced the insulin-stimulated Akt activation in the isolated caveolae (Figure 8). The condition also resulted in decreases of the amount of Akt and caveolin-3 in the caveolae, implying the retardation in translocation of Akt and caveolin-3 to caveolae from cytosol (Figures 7 and 8). Thus, it appears that the reduced active forms of Akt in caveolae modulated by insulin resistance subsequently attenuate the insulin action of glucose uptake in H9c2 cardiomyoblasts.

Carvalho *et al.,* (2000) reported the impaired phosphorylation and insulin-stimulated translocation to the plasma membrane of Akt in adipocytes from type 2 diabetic subjects. Recent studies in rat adipocytes demonstrated that cholesterol depletion, which disrupts cholesterol-rich caveolae domain in the plasma membrane, impaired insulin-stimulated Akt activation and glucose uptake (Yamamoto *et al.,* 1998; Parpal *et al.,* 2001; Karlsson *et al.,* 2002; Muller *et al.,* 2002). Thus, it is interesting that the impairment of actin remodeling by the insulin resistance condition in H9c2 cardiomyoblasts is closely related to the retardation in Akt translocation to caveolae and a decrease in the amount of phospholylated Akt in caveolae for insulin-stimulated glucose uptake. Insulin-induced actin remodeling promotes GLUT4 insertion at muscle cell membrane ruffles, and insulin-mediated GLUT4 translocation is dependent on the rearrangement of actin stress fibers in adipocytes and muscle cells (Tsakiridis *et al.,* 1994; Clodi *et al.,* 1998; Wang *et al.,* 1998; Olson *et al.,* 2001; Tong *et al.,* 2001). In addition, recent evidence for the organization of caveolin-associated membrane domains by the actin cytoskeleton and signal transduction of stretch-induced RhoA and Rac1 activation through caveolae suggest the cytoskeletal regulation of caveolae organization (Stahlhut and van Deurs, 2000; Kawamura *et al.,* 2003). It has been well established that a number of signaling molecules in diverse signal transduction are localized to caveolae and that caveolae is involved in the regulation of cellular signaling.

Thus, another implication of our finding concerns the possible alteration in the microdomain of caveolae by insulin resistance. The retardation in actin remodeling in H9c2 cells by insulin resistance might hamper the physicochemical integrity of caveolae domain in the plasma membrane. As a result, insulin triggering of glucose uptake is modulated upstream by retardation of insulin-dependent stimulation of 2-deoxy[^{3}H] glucose uptake, conceivably through impairment of insulin-stimulated translocation of phosphorylated Akt to caveolae and prevention of glucose transporter recruitment. This interpretation is consistent with previous studies reporting that disruption of caveolae domains in the plasma membrane impaired insulin-stimulated glucose uptake in rat adipocytes and 3T3L1 adipocytes (Gustavsson *et al.,* 1999; Parpal *et al.,* 2001; Karlsson *et al.,* 2002; Muller *et al.,* 2002).

In conclusion, it is apparent that insulin resistance decreases insulin-induced Akt activation in caveolae in parallel with a reduction in the translocation of phosphorylated Akt and caveoiln-3 to caveolae and actin remodeling in H9c2 cardiomyoblasts. The interrelated retardation by insulin resistance influences a downstream target of insulin signaling, namely, a decrease in glucose uptake in H9c2 cells. Thus, the modulation of caveolin-3 and Akt status in caveolae and Akt activation in caveolae play an important role in the control of the signaling pathway whereby insulin promotes glucose uptake in H9c2 cardiomyoblasts.

Acknowledgement

We would like to thank all of the members of our laboratory for their help during the course of these studies. This work was supported in part by KOSEF R01-1999-00091 and Brain Korea 21 to YP.

References

Alessi DR, Andjelkovic M, Caudwell B, Cron P, Morrice N, Cohen P, Hemmings BA. Mechanism of activation of protein kinase B by insulin and IGF-1. EMBO J 1996;15:6541-51

Bellacosa A, Testa JR, Staal SP, Tsichlis, PN. A retroviral oncogene, Akt, encoding a serine-threonine kinase containing an SH2-like region. Science 1991;254:274-7

Bickel PE. Lipid rafts and insulin signaling. Am J Physiol Endocrinol Metab 2002;282:E1-E10

Carvalho E, Eliasson B, Wesslau C, Smith U. Impaired phosphorylation and insulin-stimulated translocation to the plasma membrane of protein kinase B/Akt in adipocytes from Type II diabetic subjects. Diabetologia 2000;43:1107-15

Clodi M, Vollenweider P, Klarlund J, Nakashima N, Martin S, Czech MP, Olefsky JM. Effects of general receptor for phosphoinositides on insulin and insulin-like growth factor I-induced cytoskeletal rearrangement, GLUT4 translocation, and deoxyribonucleic acid synthesis. Endocrinology 1998; 139:4984-90

Cohen AW, Combs TP, Scherer PE, Lisanti MP. Role of caveolin and caveolae in insulin signaling and diabetes. Am J Physiol Endocrinol Metab 2003a;285:E1151-E1160

Cohen AW, Razani B, Wang XB, Combs TP, Williams TM, Scherer PE, Lisanti MP. Caveolin-1-deficient mice show insulin resistance and defective insulin receptor protein expression in adipose tissues. Am J Physiol Cell Physiol 2003b;285:C222-C235

Cong L-N, Chen H, Li Y, Zhou L, McGibbon M, Taylor S, Quon M. Physiological role of Akt in insulin-stimulated translocation of GLUT4 in transfected rat adipose cells. Mol Endocrinol 1997;11:1881-90

Czech MP, Corvera S. Signaling mechanisms that regulate glucose transport. J Biol Chem 1999;274:1865-8

Franke TF, Kaplan DR, Cantley LC. PI3K: downstream AKT blocks apoptosis. Cell 1997;88:435-7

Galbiati F, Engelman JA, Volonte D, Zhang KL, Minetti C, Li M, Hou Jr H, Kneitz B, Edelmann W, Lisanti MP. Caveolin-3 null mice show a loss of caveolae, changes in the microdomain distribution of the dystrophin-glycoprotein complex, and t-tubule abnormalities, J Biol Chem 2001;276: 21425-33

Gratton J-P, Bernatchez, P, Sessa WC. Caveolae and caveolins in the cardiovascular system. Circ Res 2004;94: 1408-17

Gustavsson J, Parpal S, Karlsson M, Ramsing C, Thorn H, Borg M, Lindroth M, Peterson KH, Magnusson KE, Stralfors P. Localization of the insulin receptor in caveolae of adipocyte plasma membrane. FASEB J 1999;13:1961-71

Ha H, Kwak HB, Lee BW, Kim HH, Lee ZH. Lipid rafts are important for the association of RANK and TRAF 6. Exp Mol Med 2003;35:279-84

Hagiwara Y, Sasaoka T, Araishi K, Imamura M, Yorifuji H, Nonaka I, Ozawa E, Kikuchi T. Caveolin-3 deficiency causes muscle degeneration in mice. Hum Mol Genet 2000;9:3047-54

Hajduch E, Litherland GJ, Hundal HS. Protein kinase B (PKB/Akt)--a key regulator of glucose transport? FEBS Lett 2001;492:199-203

Jones PF, Jakubowicz T, Pitossi FJ, Maurer F, Hemmings BA. Molecular cloning and identification of a serine/threonine protein kinase of the second-messenger subfamily. Proc Natl Acad Sci USA 1991;88:4147-75

Kahn BB. Type 2 Diabetes: When insulin secretion fails to compensate for insulin resistance. Cell 1998;92:593-6

Karlsson M, Thorn H, Parpal S, Stralfors P, Gustavsson J. Insulin induces translocation of glucose transporter GLUT4 to plasma membrane caveolae in adipocytes. FASEB J 2002;16:249-51

Kawamura S, Miyamoto S, Brown JH. Initiation and transduction of stretch-induced RhoA and Rac1 activation through caveolae: cytoskeletal regulation of ERK translocation. J Biol Chem 2003;278:31111-7

Kawanaka K, Han D-H, Gao J, Nolte LA, Holloszy JO. Development of glucose-induced insulin resistance in muscle requires protein synthesis. J Biol Chem 2001;276:20101-7

Kim B-W, Choo H-J, Lee J-W, Kim J-H, Ko Y-G. Extracellular ATP is generated by ATP synthase complex in adipocyte lipid rafts. Exp Mol Med 2004;36:476-85

Kim S, Pak Y. Caveolin-2 regulation of the cell cycle in response to insulin in Hirc-B fibroblast cells. Biochem Biophys Res Comm 2005;330:88-96

Kimes BW, Brandt BL. Properties of a clonal muscle cell line from rat heart. Exp Cell Res 1976;98:367-81

Kohn AD, Barthel A, Kovacina KS, Boge A, Wallach B, Summers SA, Birnbaum MJ, Scott PH, Lawrence Jr JC, Roth RA. Construction and characterization of a conditionally active version of the ser/thr kinase Akt. J Biol Chem 1998; 273:11937-43

Kotani K, Ogawa W, Matsumoto M, Kitamura T, Sakaue H, Hino Y, Miyake K, Sano W, Akimoto K, Ohno S, Kasuga M. Requirement of atypical protein kinase Cλ for insulin stimulation of glucose uptake but not for Akt activation in 3T3-L1 adipocyte. Mol Cell Biol 1998;18:6971-82

Levy AP, Levy NS, Goldberg MA. Post-transcriptional regulation of vascular endothelial growth factor by hypoxia. J Biol Chem 1996;271:2746-53

Mueckler M. Insulin resistance and the disruption of GLUT4 trafficking in skeletal muscle. J Clin Invest 2001;107:1211-3

Muller G, Hanekop N, Wied S, Frick W. Cholesterol depletion blocks redistribution of lipid raft components and insulin-mimetic signaling by glimepiride and phosphoinositolglycans in rat adipocytes. Mol Med 2002;8:120-36

Nelson BA, Robinson KA, Buse MG. High glucose and glucosamine induce insulin resistance via different mechanisms in 3T3-L1 adipocytes. Diabetes 2000;49:981-91

Olson AL, Trumbly AR, Gibson GV. Insulin-mediated GLUT4 translocation is dependent on the microtubule network. J Biol Chem 2001;276:10706-14

Parpal S, Karlsson M, Thorn H, Stralfors P. Cholesterol depletion disrupts caveolae and insulin receptor signaling for metabolic control via insulin receptor substrate-1, but not for mitogen-activated protein kinase control. J Biol Chem 2001; 276:9670-8

Razani B, Woodman SE, Lisanti MP. Caveolae: From cell biology to animal physiology. Pharmacol Rev 2002;54: 431-67

Rybin VO, Xu X, Lisanti MP, Steinberg SF. Differential targeting of beta-adrenergic receptor subtypes and adenylyl cyclase to cardiomyocyte caveolae. J Biol Chem 2000; 275:41447-57

Schlegel A, Volonte D, Engelman JA, Galbiati F, Mehta PS, Zhang X, Scherer PE, Lisanti MP. Crowded little caves: structure and function of caveolae. Cell Signal 1998;10: 457-63

Sharma PM, Egawa K, Huang Y, Martin JL, Huvar I, Boss GR, Olefsky JM. Inhibition of phosphatidylinositol 3-kinase activity by adenovirus-mediated gene transfer and its effect on insulin action. J Biol Chem 1998;273:18528-37

Song KS, Li S, Okamoto T, Quilliam LA, Sargiacomo M, Lisanti MP. Co-purification and direct interaction of ras with caveolin, an integral membrane protein of caveolae microdomains. Detergent-free purification of caveolae membranes. J Biol Chem 1996;271:9690-6

Stahlhut M, van Deurs B. Identification of filamin as a novel ligand for caveolin-1: evidence for the organization of caveolin-1-associated membrane domains by the actin cytoskeleton. Mol Biol Cell 2000;11:325-37

Stephens JM, Pilch PF. The metabolic regulation and vesicular transport of GLUT4, the major insulin-responsive glucose transporter. Endocrine Rev 1995;16:529-46

Tanti JF, Grillo S, Gremeaux T, Coffer PJ, Van Obberghen E, Le Marchand-Brustel Y. Potential role of protein kinase B in glucose transporter 4 translocation in adipocytes. Endocrinology 1997;138:2005-10

Thomson MJ, William MG, Frost SC. Development of insulin resistance in 3T3-L1 adipocytes. J Biol Chem 1997;272: 7759-64

Tong P, Khayat ZA, Huang C, Patel N, Ueyama A, Klip A. Insulin-induced cortical actin remodeling promotes GLUT4 insertion at muscle cell membrane ruffles. J Clin Invest 2001;108:371-81

Tsakiridis T, Vranic M, Klip A. Disassembly of the actin network inhibits insulin-dependent stimulation of glucose transport and prevents recruitment of glucose transporters to the plasma membrane. J Biol Chem 1994;269:29934-42

Ueki K, Yamamoto-Honda R, Kaburagi Y, Yamauchi T, Tobe K, Burgering BT, Coffer PJ, Komuro I, Akanuma Y, Yazaki Y, Kadowaki T. Potential role of protein kinase B in insulin-induced glucose transport, glycogen synthesis, and protein synthesis. J Biol Chem 1998;273:5315-22

Uittenbogaard A, Shaul PW, Yuhanna IS, Blair A, Smart EJ. High density lipoprotein prevents oxidized low density protein-induced inhibition of endothelial nitric-oxide synthase localization and activation in caveolae. J Biol Chem 2000; 275:11278-83

Wang QH, Bilan PJ, Tsakiridis T, Hinek A, Klip A. Actin filaments participate in the relocalization of phosphatidylinositol 3-kinase to glucose transporter-containing compartments and in the stimulation of glucose uptake in 3T3-L1 adipocytes. Biochem. J 1998;331:917-28

Yamamoto M, Toya Y, Schwencke C, Lisanti MP, Myers Jr MG, Ishikawa Y. Caveolin is an activator of insulin receptor signaling. J Biol Chem 1998;273:26962-8

Yu B, Poirier LA, Nagy LE. Mobilization of GLUT4 from intracellular vesicles by insulin and K(+) depolarization in cultured H9c2 myotubes. Am J Physiol 1999;277:E259-E267